



## Strathprints Institutional Repository

**Ledwon, Przemyslaw and Thomson, Neil and Angioni, Enrico and Findlay, Neil J. and Skabara, Peter J. and Domagala, Wojciech (2015) The role of structural and electronic factors in shaping the ambipolar properties of donor-acceptor polymers of thiophene and benzothiadiazole. RSC Advances, 5 (94). pp. 77303-77315. ISSN 2046-2069 , <http://dx.doi.org/10.1039/c5ra06993a>**

This version is available at <http://strathprints.strath.ac.uk/55930/>

**Strathprints** is designed to allow users to access the research output of the University of Strathclyde. Unless otherwise explicitly stated on the manuscript, Copyright © and Moral Rights for the papers on this site are retained by the individual authors and/or other copyright owners. Please check the manuscript for details of any other licences that may have been applied. You may not engage in further distribution of the material for any profitmaking activities or any commercial gain. You may freely distribute both the url (<http://strathprints.strath.ac.uk/>) and the content of this paper for research or private study, educational, or not-for-profit purposes without prior permission or charge.

Any correspondence concerning this service should be sent to Strathprints administrator: [strathprints@strath.ac.uk](mailto:strathprints@strath.ac.uk)

# The role of structural and electronic factors in shaping the ambipolar properties of donor-acceptor polymers of thiophene and benzothiadiazole

Przemyslaw Ledwon <sup>a</sup>, Neil Thomson <sup>b</sup>, Peter Skabara <sup>b</sup>, Wojciech Domagala <sup>a,\*</sup>

a – Silesian University of Technology, Faculty of Chemistry, Department of Physical Chemistry and Technology of Polymers, ul. Marcina Strzody 9, 44-100 Gliwice, Poland

b – University of Strathclyde, Department of Pure and Applied Chemistry, 295 Cathedral Street, Glasgow G1 1XL, United Kingdom

## Abstract

The influence of the donor unit of D-A type of  $\pi$ -conjugated organic materials on optical and electrochemical properties is studied. The stability of organic materials is limiting factor in commercial applications of these type of materials. Report usually focus on short time device performance which is worsened in short time. One of the main reason is poor stability of organic compounds during doping. Herein the influence of different donor units with benzothiadiazole as acceptor units on p- and n-doping is taken to consideration. The UV-Vis-NIR and EPR spectroelectrochemical measurement help in the elucidation of different effects determining the ambipolar properties of these polymers. The inductive and resonance effects are well known. Herein additional steric effect leading to rigidification of polymer chain and stabilization of n- and p-doped polymers is observed. The proper combination of these units is crucial to obtain better D-A polymers.

**Keywords:** conducting polymers, donor – acceptor, thiophene, benzothiadiazole, electrochemistry, spectroelectrochemistry,

## 1. Introduction

Numerous papers have been reported the influence of the side groups. Usually the side groups such as alkyl chains are incorporated in order to improve solubility of conjugated molecules in organic medium. Other substituents including several functional groups are incorporated to modified physical properties such as energy levels, absorption, emission and morphology[1,2]. Side groups often lead to improved self ordering with enhanced charge mobility[3] in other cases they worsen the electric conductivity due to steric hindrance. HOMO and LUMO orbital energy levels and hence energy gap can be tuned mainly own to different inductive or resonance effects. Electron withdrawing groups lower orbital energy levels while electron donating groups raise orbital energy levels. First group of

substituents include aldehyde[4], malanonitrile[5], alkylsulfonyl[6] and fluoroalkyl[7] groups. The latest include alkoxy[8], alkyloamino and acetate groups.

A special kind of interaction caused by side groups is observed in the case of poli(3,4-etyleno-1,4-dioksytiofen) (PEDOT). A strong interaction between O and S atoms of neighboring EDOT units leads to rigitation of polymers chain effectively reinforcement the effective conjugation length[9]. This effect resulted in the great electrochemical and optical properties has contribution to commercial applications of PEDOT[10]. A sulphur derivative 3,4-etyleno-1,4-ditiatiofen (EDTT) present similar redox properties to EDOT[11], however redox properties of their polymers are more divergent due to weaker interaction between S atoms[9].

The donor-acceptor (D-A) structure in conjugated polymers has been introduced in recent years to afford polymers with improved properties. This type of  $\pi$ -conjugation organic materials consist of electron-rich and electron-deficient units[12]. Some D-A polymers exhibited remarkable properties such as broad and strong absorption, narrow band gap, fast and reversible color changing, high conductivity[13–16]. In addition these groups of polymers present high stability during doping process with different charge carriers during the redox process that is considered to be one of the main processes to decrease the distance between HOMO and LUMO energy levels[17]. This has pushed them to be employed in several electronic applications such as photovoltaic devices [17–19] organic field effect transistors[13] and electrochromic devices for instance smart windows and mirrors [15,20,21].

The benzothiadiazole (BT) molecule is considered to be one of the richest electron acceptor units used to modified the LUMO energy level in D-A type of polymers[22]. An electron-deficient BT unit has been attached to electron rich molecules such as thiophene derivatives resulting in unique optical and electrochemical properties[23–27]. When BT is incorporated with electron donor units, the extension of the conjugated length appears, due to the occurrence of intarmolecular charge transfer (ICT) in D-A structure[28,29]. These conjugated materials have been synthesized and characterized to enhance the electrochemical and optical properties for instance low HOMO-LUMO gap values, fast switching time, high optical contrast and high conductivity[19,30,31].

Toppare *et al.* have investigated D-A materials based on 3,4-ethylenedioxythiophene (EDOT) and BT as donor and acceptor units respectively, that exhibited an extremely low band gap and high stability under redox cycling[32–35]. Therefore these materials are candidates for electrochromic applications owing to their fast switching and reversible change between green and transmissive light blue in the neutral and doped states, respectively. Similarly, El-Shehawy *et al* investigated a series of D-A alternating conjugated copolymers based on hexylthiophene and BT units[28]. From these studies, broader absorption bands with modified HOMO and LUMO orbital energy values have been demonstrated. Thiophene derivatives have been studied previously and they have shown exceptional electroactive behavior in both monomer and polymer cases. These materials acted as a conducting polymer own to its properties such as low oxidation potential and high conductivity[36].

In this paper, five monomers (**1-5**) and their polymers have been characterized. Polymers have been prepared electrochemically and studied using electrochemical and spectroelectrochemical experiments. Monomers (**1-5**) contain a benzothiadiazole core, attached to two side units which are thiophene, 3-hexylthiophene, 3-dodecylthiophene, EDOT and EDTT.

## **2. Synthesis and experimental**

### **2.1 Materials and synthesis**

The structures of monomers are shown in Figure 1. 4,7-bis(thiophen-2-yl)-2,1,3-benzothiadiazole (**1**) was purchased from TCI Europe.

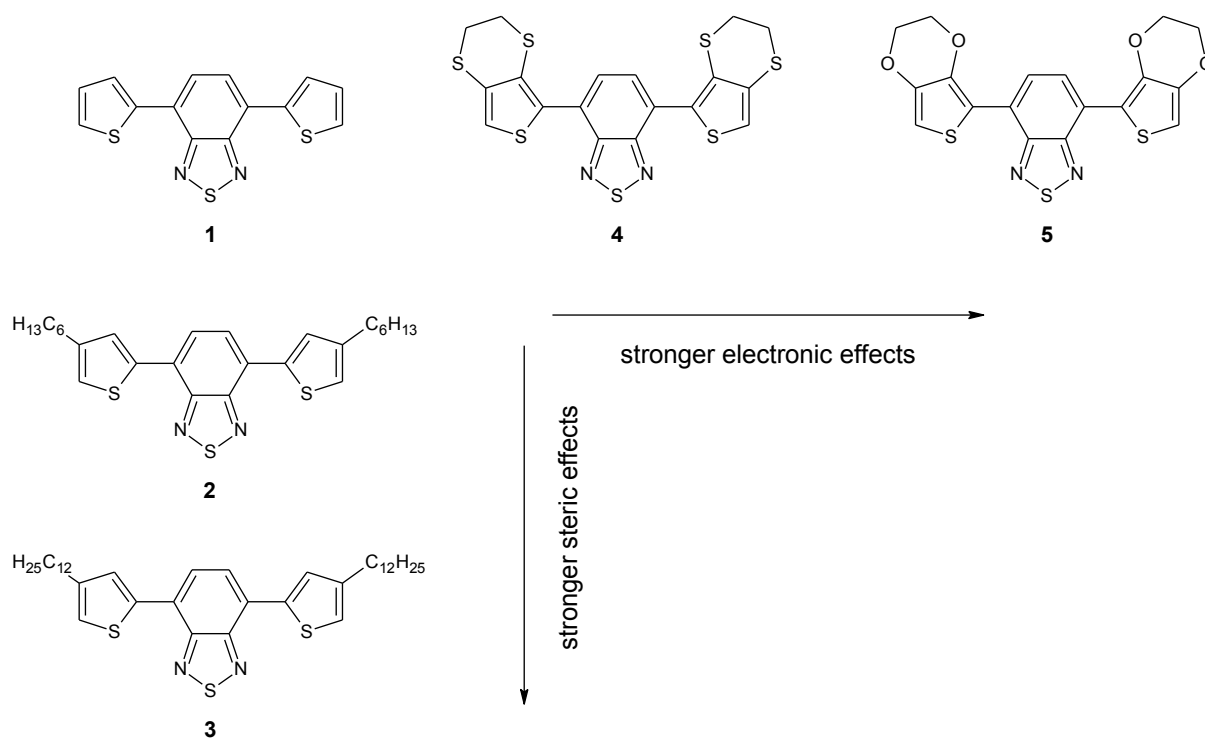
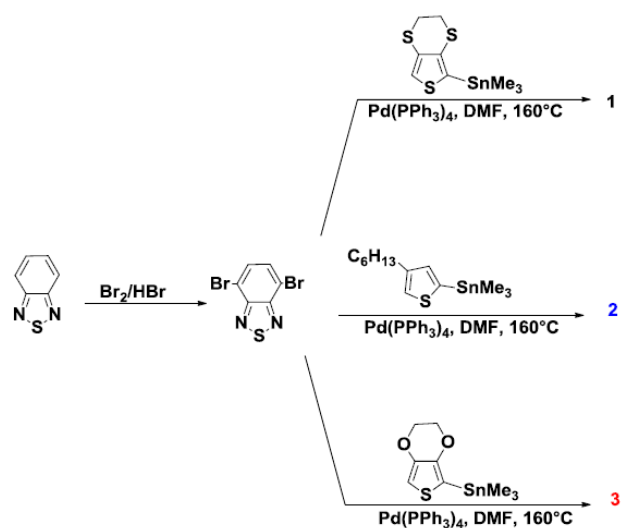


**Figure 1.** Investigated monomers 1-5.

Compounds 2-5 were synthesized according to the procedure illustrated at scheme 1. Benzothiadiazole was dibrominated using HBr and Br<sub>2</sub>. 3,4-Ethylenedioxythiophene (EDOT), 3,4-ethylenedithiothiophene (EDTT) and 3-hexylthiophene were stannylated *via* lithiation followed by the addition of Me<sub>3</sub>SnCl at -78°C. Compounds (2-5) were obtained in good yield (78, 82 and 67% respectively) using microwave assisted Stille cross coupling at 160°C and Pd(PPh<sub>3</sub>)<sub>4</sub> as the catalyst.<sup>14</sup>



**Scheme 1.** The synthesis of compounds 2 to 5

## 2.2 Electrochemistry

Electrochemical measurement were made in a classic three electrodes assemble with Pt disc electrode as the working electrode, Pt spiral as the counter electrode and Ag wire as pseudo-reference electrode. All experiments were made in dichloromethane (DCM) (Sigma-Aldrich, for HPLC), acetonitrile (ACN) (Sigma-Aldrich, for HPLC), tetrahydrofuran (THF) (Alfa Aesar, 99,5 Extra dry) or in mixed DCM/ACN solutions. Tetrabutylammonium hexafluorophosphate ( $\text{Bu}_4\text{NPF}_6$ ) (TCI) 0.1 M was used as the supporting electrolyte. All solutions were deoxygenated by bubbling 15 minutes with Ar before measurement. All measurements are referenced versus ferrocen redox couple. Electrochemical measurement were made using CH Instruments 620.

### 2.3 Spectroelectrochemistry

Polymer films were electrochemically deposited directly on ITO electrode. After synthesis, polymers were rinsed with fresh solvent, immersed in 0.1M  $\text{Bu}_4\text{NPF}_6/\text{ACN}$  electrolyte and electrochemically dedoped. Optical spectroelectrochemical cell adapted for simultaneous EPR, UV-vis-NIR and electrochemical measurement was used. The spectroelectrochemical cell consist of cylindrical quartz tube and intermediate EPR signal-free quartz flat part. 0.3 mm ITO electrodes were inserted to the 0.5 mm slot in the flat part. Teflon coated Ag pseudo-reference electrode was assemble next to the ITO electrode. Pt spiral counter electrode was assemble in the cell tube bottom part. Ar bubbling of electrolyte solution was performed in the cell tube top part continuously during spectroelectrochemical measurement.

EPR measurements were carried out using JEOL JES FA 200, X-band CW-EPR spectrometer, operating at 100 kHz field modulation, while UV-vis-NIR measurements were carried out using a Ocean Optics QE65000 and NirQuest512 spectrometers coupled with DH-BAL200 light source. EPR spectrometer were equipped with optical resonator. Light for UV-Vis-NIR measurement was provided and collected by optical fibers. Potential were applied by Autolab PGSTAT100N potentiostat.

EPR and UV-Vis-NIR spectra have been collected *in situ* at stepwise applied potentials in the anodic range during p-doping and dedoping. This procedure was changed in the cathodic range due to different characteristic of reduction processes and difference in electrochemical stability of n-doped polymers.

The spectroelectrochemical measurement of p-doping and dedoping were made after reaching the equilibrium which takes several seconds. In this state further changes at EPR or UV-Vis-NIR spectra are not observed. EPR spectra were measured at every potential twice with two different parameters to ensure the best conditions to estimate g-value, relative spin concentration and linewidth ( $\Delta B_{pp}$ ). The relative concentrations of paramagnetic species was determined by double integration of the first-derivative EPR spectra with baseline correction. The g-factor was estimate using Mn marker.  $\Delta B_{pp}$  of EPR signal was estimated from spectra recorded with modulation amplitude equal or lower than 0.25 of the narrowest  $\Delta B_{pp}$ . The high signal to noise ratio is required from measurement aimed at

estimation of concentrations of paramagnetic species. This can be achieved by setup high modulation amplitude. To estimate the best signal to noise ratio the same modulation amplitude was used, being chosen as 1.5 of the narrowest  $\Delta B_{pp}$ . This value was in the linear range of dependence of signal intensity estimated from double integration of EPR signal and modulation amplitude. Second EPR spectra was recorded at modulation amplitude chosen as 0.25 of the narrowest  $\Delta B_{pp}$ . At this parameter only negligible deformation of EPR line shape is observed and hence the linewidth of EPR signal can be estimated[37].

The procedure of spectroelectrochemical measurement during n-doping and dedoping was different. The reduction potential has been set from CV reduction curves as reduction potential peak. In contrary to p-doping the equilibrium in the n-doping was achieved after much longer time reaching several minutes. Spectra were recorded after reaching the electrochemical equilibrium. EPR spectra were recorded only at modulation amplitude chosen as 0.25 or lower of the narrowest  $\Delta B_{pp}$  own to better signal to noise ratio than in oxidation process.

### 3. Results

#### 3.1 Photophysical properties of monomers.

The absorption spectra of monomers **1-5** recorded in DCM solution are shown in Figure 2. The absorption spectra of all compounds are similar in shaped with at least three peaks. The lowest energy peak can be assigned to intramolecular charge transfer (ICT)[29]. Higher energy peaks correspond to the  $\pi-\pi^*$  transitions at main chain. The absorption spectrum of **1** exhibits peaks at 443 nm, 307 nm and 253 nm. The spectra of monomers **2** and **3** present bathochromic shift with peaks at 456 nm, 311 nm and 258 nm as a results of inductive electron donating effect of alkyl substituents. The absorption peaks of compound **54** are located at 448 nm, 301 nm, and 252 nm while for compound **45** are located at 479 nm, 323 nm, 263 nm compared to compounds **2** and **3**. The bathochromic shift of compound **45** arise from mix inductive and mesomeric effects of ethylenedioxy substituent[38].

The ICT is commonly observed in the D-A type of conjugated molecules both low molecular weight materials and polymers containing in their structure BT and different thiophene derivative units[39–45]. Characteristic properties of this type of molecules such as low energy gap and strong broad absorbance are important in the photovoltaic application[44,45].

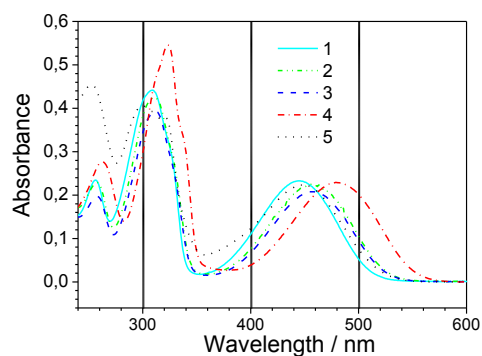


Figure 2 UV-Vis spectra of  $1 \cdot 10^{-3}$  M compounds **1-5** solutions in DCM.

### 3.2 Electrochemistry.

The electrochemistry of the monomers and polymers was achieved by cyclic voltammetry in an DCM, ACN, THF or mixed DCM/ACN solutions. Different solvents were chosen due to significant differences in the solubility of studied compounds and different electrochemical window of solvents in anodic and cathodic range.

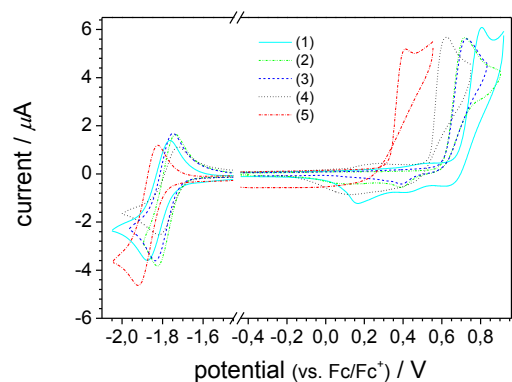


Figure 3 Cyclic voltammetry of compounds **1-5** in cathodic and anodic range; concentration  $1 \cdot 10^{-3}$  M; 0.1 M  $\text{Bu}_4\text{NPF}_6/\text{DCM}$ ; scan rate  $0.1 \text{ V} \cdot \text{s}^{-1}$ .

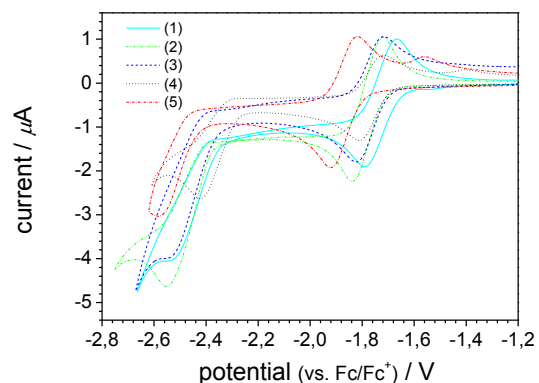


Figure 4 Cyclic voltammetry of compounds **1-5** in extended cathodic range;  $1 \cdot 10^{-3}$  M solutions in 0.1 M  $\text{Bu}_4\text{NPF}_6/\text{THF}$ ; scan rate  $0.1 \text{ V} \cdot \text{s}^{-1}$ .



Cyclic voltammetry curves performed in DCM exhibit quasireversible redox pair in cathodic range and irreversible peak in the anodic range (Figure 3). A redox pair in the cathodic range is attributed to the reversible reduction of the BT unit. BT is known to be a strong electron acceptor. THF was chosen to exceed the potential range in cathodic range due to broader potential window in this range. Cyclic voltammetry performed in THF present two well separated reduction peaks, first reversible and second irreversible reduction peak (Figure 4). Results are summarized in the Table 1.

The difference of oxidation potential values in the monomers is attributed to the different side group effects. Monomer **45** has the lowest potential compared with other monomers. It is consistent with earlier reports about the reducing the oxidation potential of EDOT compared to thiophene units.

Table 1 Redox and electronic properties of monomers and polymers. IP – ionization potential estimated from equation  $IP = 5.1 + E_{onset}^{ox}$ ; EA - electron affinity estimated from equation  $EA = 5.1 + E_{onset}^{ox}$ ;  $E_g^{el}$  - electrochemical energy gap estimated from equation  $E_g^{el} = IP - EA$ ;  $E_g^{op}$  – optical energy gap estimated from equation  $E_g^{op} = 1240/\lambda_{onset}$  where  $\lambda_{onset}$  is the onset of absorption edge.

compound	$E_{onset}^{ox}$ [V]	$E_{onset}^{red}$ [V]	IP [eV]	EA [eV]	$E_g^{el}$ [eV]	$E_g^{op}$ [eV]
1	0.69	-1.74	5.8	3.4	2.4	2.44
poly1	0.34	-1.52	5.4	3.6	1.8	1.63
2	0.62	-1.71	5.7	3.4	2.3	2.36
poly2	0.30	-1.57	5.4	3.5	1.9	1.61
3	0.62	-1.71	5.7	3.4	2.3	2.36
poly3	0.36	-1.60	5.5	3.5	2.0	1.57
5	0.53	-1.70	5.6	3.4	2.2	2.39
poly5	0.30	-1.4	5.4	3.8	1.7	1.75
4	0.33	-1.77	5.4	3.3	2.1	2.25
poly4	-0.68	-1.66	4.4	3.4	1.0	1.26

All monomers present good solubility in DCM and THF. However the electrochemical polymerization of **2** and **3** in these solvents lead to formation of soluble products. ACN is poor solvent for compounds with long alkyl substituents, the elongation of alkyl chain worsen the solubility. These are the reasons of electropolymerization performance of compounds **2** and **3** in mix DCM and ACN solution. Proper rate of these solvents ensure the 1mM solubility of compounds **2** and **3** with simultaneous insolubility of products formed as a result of electrooxidation of monomers.

Cyclic voltammetry recorded during reverse scanning for the first oxidation peak is presented at Figure 5. In all cases below oxidation potential of monomers at every subsequent scan an increase of current is observed. Simultaneously the electrochromic film deposit at working electrode. Redox peaks at lower potentials appear as a results of formation of compounds with longer conjugation at the electrode surface. These results indicate the occurrence of electrochemical polymerization according to well known electrodeposition mechanism of conjugated polymers[46].

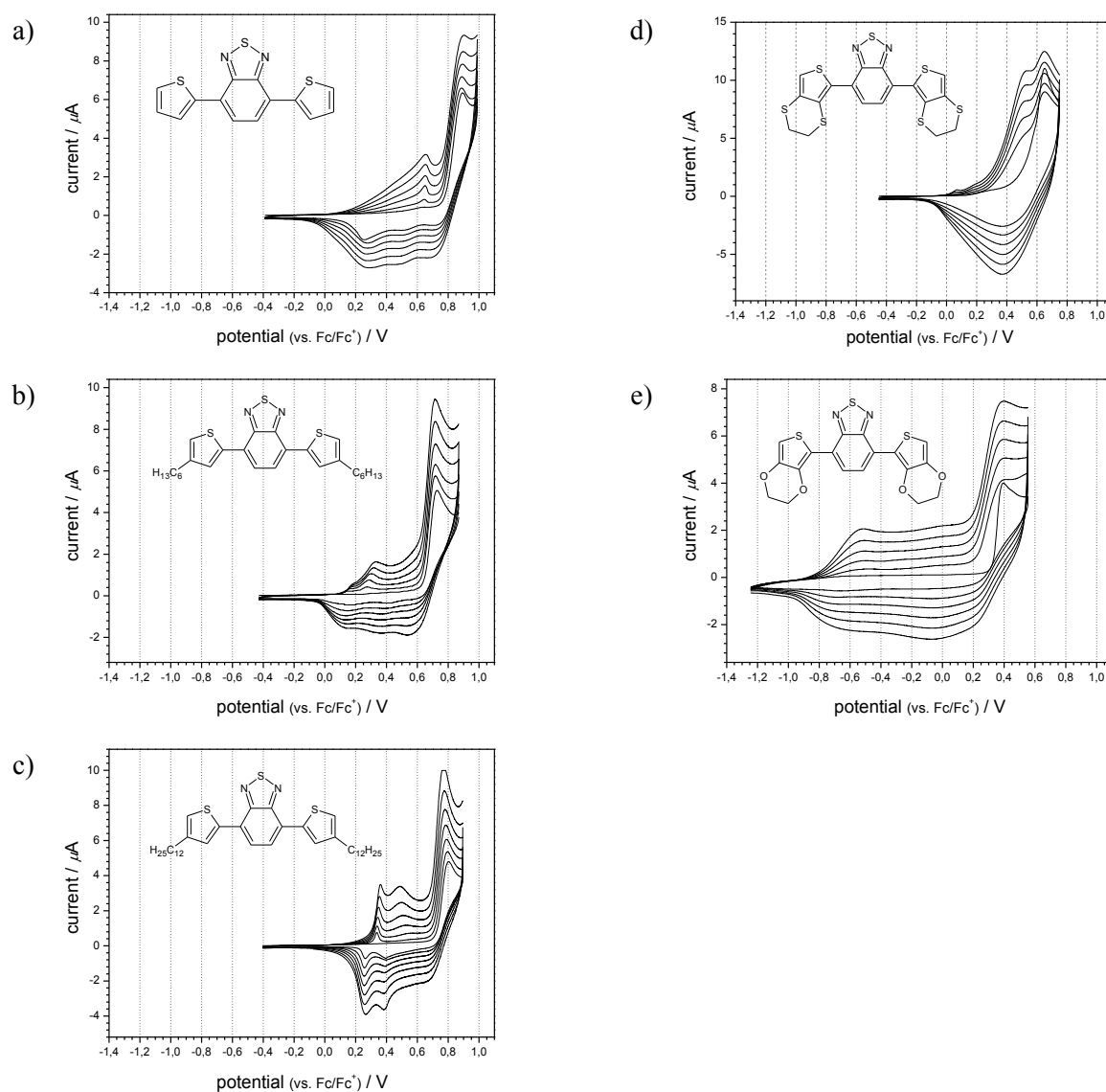


Figure 5 Cyclic Voltammetry recorded during polymerization of compounds **1-5: 2** in DCM:ACN 1:1(a); **3** in DCM:ACN 1:3 (b); **54** (c) and **45** in DCM (d). 0.1 M Bu<sub>4</sub>NPF<sub>6</sub> as supporting electrolyte. Scan rate 0.1 V·s<sup>-1</sup>.

The cyclic voltammetry of polymer films were made in ACN due to their insolubility in this solvent (Figure 6). The characteristic of voltammetric curves depends on structure of thiophene

derivative units. Detailed analysis reveals that all polymer can be reversibly. Considering the influence of alkyl substituents on the redox properties the current ratio between n-doping and p-doping was taken into account. At CV of **poly1** sharp and reversible reduction is observed. The current ratio between n- and p-doping clearly decrease in order **poly1**; **poly2**; **poly3**. The increased length of alkyl substituents worsen the n-doping ability of polymer films. It can be explained as a result of moving apart of polymer chains with increased volume of alkyl groups and hence reduction of charge carriers hopping between electron acceptor moieties.

The CV of **poly4** exhibit the strong shift to lower potential values of oxidation onset potential compared to **poly1** and its alkyl derivatives. This characteristic effect in the EDOT derivative polymers is mainly attributed to the intramolecular chalcogen–chalcogen interactions. A strong O··S intramolecular interaction between neighbor EDOT units lead to rigidity of polymer chain and increase of effective conjugated length[9]. Similar effect is much weaker between S··S intramolecular interaction in the case of **poly5**. Based on basic redox properties determined from CV further spectroelectrochemical measurements were made.

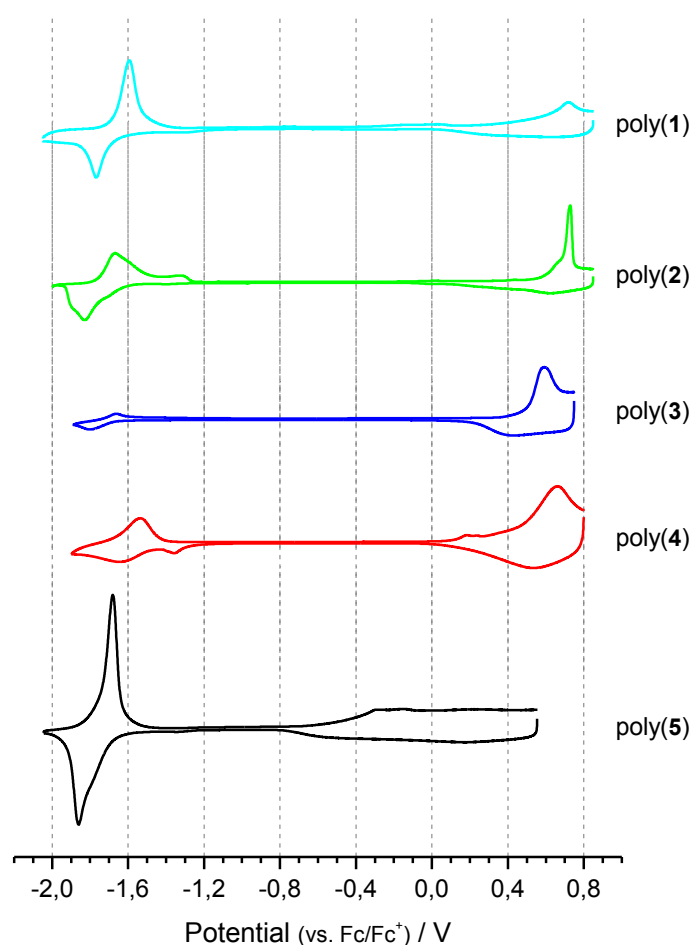


Figure 6 Cyclic Voltammetry of polymer films recorded in 0.1 M Bu<sub>4</sub>NPF<sub>6</sub> / ACN . Scan rate 0.1 Vs<sup>-1</sup>.

### 3.3 Electronic properties

The electronic properties of monomers and polymers were estimated from cyclic voltammetry and UV-Vis spectra. The ionization potential (IP) were calculated from the onsets of the first oxidation peak and the electron affinity (EA) from the onsets of the first reduction peak. IP and EA are associated with HOMO and LUMO level respectively. From difference between IP and EA the electrochemical band gap  $E_g^{el}$  was estimated. Optical HOMO-LUMO band gap  $E_g^{op}$  was estimated from the intersection of the line based on the edge of the spectrum and baseline. The energy of onset of the absorption edge gives  $E_g^{op}$  for the monomers and polymers. Results are collected in Table 1.

Monomer **1** have IP value of 5.8 eV. The IP value of **45** is equal to 5.4 eV as a results of electron donating effect of 3,4-etyleno-1,4-dioksyl substitution and additional rigidity effect. Similar much weaker effect present monomers **2**, **3** and **54** with IP equal to 5.7 eV. All monomer present similar EA values in the range from 3.3 eV up to 3.4 eV.  $E_g^{el}$  and  $E_g^{op}$  are similar in value, their difference not exceed 0.2 V. In both cases monomer **45** has the lowest value.

In all cases of polymers the decrease of EA and increase of IP compared to monomers is observed. IP of poly**1**, poly**2**, poly**3** and poly**54** is lower than monomers approximately 5.4 eV. Compared to monomers only 0.3 eV shift is observed. Much greater difference is observed in the case of compound **45** which oxidative electrodeposition results in the product with EA of 4.4 eV. It is characteristic effect observed for EDOT and PEDOT due to strengthened of influence of O...S intramolecular interaction in the polymer structure.

Compared to pure PEDOT only slightly change of the IP occurs. The conjugation between biEDOT units formed as a results of electrochemical oxidation of monomers is not interrupt at BT units. It is explained by conjugation through p-benzoquinoidal type of structure at BT moiety. The influence of substitution and polymerization at EA values is smaller however observed. It is typical for compound with BT acceptor unit, which LUMO is localized mainly at 1,2,5-thiadiazole moiety.[47]

Calculated  $E_g^{op}$  values were found to be 2.44, 2.33, 2.33, 2.23 and 2.37 eV for monomers **1-5** respectively.  $E_g^{el}$  was estimated to be 2.3 eV for **2** and **3**, 2.2 for **54** and 2.1 for **45**. Greater differences between studied compounds were found in the case of polymers. The trend of  $E_g^{el}$  and  $E_g^{op}$  of polymers is similar to monomers. In all cases of polymers the narrowing of those values is observed. The narrowest energy gap characterize poly(**45**) mainly as a results of change of HOMO level. The differences between  $E_g^{el}$  and  $E_g^{op}$  for polymers can be explained as effect of additional electrochemical processes taking place at the working electrode such as reorganization of the polymer film structure and different overpotential components.

### 3.4 EPR/UV-Vis-NIR spectroelectrochemistry.

The role of structure of the electron donor units on properties of D-A type of conjugated polymers were investigated by detailed triplet EPR/UV-Vis-NIR spectroelectrochemistry. EPR and UV-Vis-NIR spectra have been collected *in situ* at stepwise applied potentials according to procedure described in the experimental section.

#### *p-Doping*

Starting from the potential at which polymers were in their neutral form the potential was gradually increased. The electrochemical p-doping were performed up to the potential estimated from CV at which polymers were stable during multiple p-doping and dedoping. In measurement conditions electrochemical instability begins after exceeding of this potential.

Selected EPR spectra of **poly2** electrodeposited at ITO electrode are shown at Figure 7. Spectrum recorded at 0 V exhibit small intensity EPR signal. Signal begins to increase at potential slightly below  $E_{onset}^{ox}$ . This is result of different measurement conditions potentiodynamic during cyclic voltammetry and potentiostatic during *in situ* EPR measurement. In the p-doping half cycle the EPR lines change their intensity and linewidth. The basic characteristic of other studied polymers is similar. The increase of EPR line intensity at the beginning of the oxidation process is observed for all four polymers. The differences occurring mainly at higher p-doping levels were analyzed in details.

Simultaneously UV-Vis-NIR spectra were recorded (Figure 8). UV-Vis-NIR spectra of polymers in their neutral state are similar in shape although the transition energy is clearly dependent on the polymer structures. The UV-Vis spectra of all polymers begin to change at the beginning of oxidation. New absorption bands appear in the lower energy range. The formation of these new transitions is associated with formation of well known charge carriers at conjugated polymer backbone. At Figure 8 the difference spectra are also shown in order to better characterize redox processes occurring at different p-doping levels. Recorded UV-Vis-NIR changes were compared with data obtained from EPR spectral analysis.

First aspect taken into consideration is the influence of alkyl substituents on p-doping process.  $E_{onset}^{ox}$  is similar for **poly1** and its alkyl derivatives **poly2** and **poly3**. At the beginning of oxidation the relative concentration of spins increase sharply (Figure 9). Simultaneously the formation of two broad absorption band at approximately 800 nm and 1400 nm is observed. At higher p-doping levels new band appears. The overlapping of different electron transitions and simultaneous increase of different peaks occur in broad potential ranges. At high doping level these changes of transition bands correlate with changes of relative spin concentration. The relative spin concentration increase up to 0.75 V (**poly1**), 0.7 V (**poly2**) and 0.58 V (**poly3**). In these potential ranges different electron transitions bands increase. After exceeding of these potentials the increase of intensity of transition band located at 1200 nm dominate at UV-Vis-NIR spectra. Simultaneously the relative spin concentration begins to decrease.

The comparison of p-doping of polythiophene D-A type derivatives with common polythiophenes reveals similarities[48]. The formation of spin bearing molecules with g-factor 2.0023 at the beginning of oxidation and two strong absorption bands indicate formation of polarons. At higher doping level the simultaneous appearance and increase of different overlapping absorption bands and increase of relative spin concentration indicate simultaneous formation of polarons and spinless species. The equilibrium between both type of charge species occur in this broad potential range. Their ratio change with increased potential as can be seen at UV-Vis-NIR spectra. The g-value slightly shift up to 2.0026 (**poly1**) and 2.0025 (poly2 and poly3) indicating change of the radical surrounding with increasing doping level. Finally only spinless species with only one transition band are generated. Commonly spinless species are explained by bipolaron, dicationic interchain  $\pi$ -dimers or  $\sigma$ -dimers model[46,48,49]. The correctness of those models is the subject of unresolved debate from few decades.

Analyzing the electrochemical dedoping the hysteresis in number of spin bearing species is observed. This phenomenon is also observed at CV. In the case of electrochemistry of conjugated polymers in the solid state the hysteresis is often observed and their explanation is still meter of discussion. It is interpreted by different kinetic and thermodynamic effects[46]. Initial explanations include charge diffusion during charging and discharging or conformation changes. However therodynamic explanation focus on formation of interchain energetically more stable  $\sigma$ -dimers with more negative redox potential than neutral polymer, spin pairing into  $\pi$ -dimers[50] or the stability of quinoid structure of bipolaron species[51].

The p-doping and dedoping of **poly54** also takes place with formation of polarons at the beginning of oxidation and spinless species at higher potentials. Characteristic polaron peaks are located at approximately 800 nm and 1500 nm, spinless species at approximately 1150 nm. EPR signal of generated **poly54** radical is centered at g-value 2.0038 at low doping levels and 2.0042 at high doping level. These values are significantly different comparing to **poly1** and free electron value  $g=2.0023$ . This indicate great contribution of the sulfur atoms to the radical cation orbital in oxidized **poly54**.

The careful inspection of **poly45** reveal more complex course of concentration of paramagnetic species than taking place in other studied polymers. In this point we also compare obtained results with previously reported by our group PEDOT doping[52]. The strong shift of  $E_{onset}^{ox}$  to low potential values observed in PEDOT voltammetry (approximately -0.9 V)[52] is maintained in **poly45** voltametric characteristic (-0.68 V). Compared to other studied polymers its revealed as shift of  $E_{onset}^{ox}$  by approximately 0.9 V. The CV of **poly45** and related concentration spin density is slightly shifted to more positive potentials than in the case of PEDOT. The trend at the beginning of doping is similar with increase of spin concentration up to -0.45 V. In this range at the UV-Vis-NIR spectra the overlapping of the neutral polymer transitions and first strong polaron transition is observed. After exceeding this potential the overlapping of more transition bands can be distinguished. The relative

concentration spin density fluctuated and then slightly increase in contrast to PEDOT. The spin density of PEDOT after reaching -0.4 V decrease monotonously. This is also reflected in CV of both polymers. The current at CV of **poly45** after exceeding of the first distinguishable peak at approximately -0.3 V slightly decrease and then increase in contrast to PEDOT CV at which monotonous decrease is observed. This can be attributed to the superposition of several redox states characteristic in conjugated polymers with long chain length. The presence of several redox states can be linked to formation of different charge carriers in crystalline and amorphous polymer phase. Similar interpretation was proposed and widely studied for electrochemically generated PEDOT[52].

In order to elucidate the character of spin bearing carriers in **poly45** the changes of linewidth of EPR signal and g-factor were estimated (Figure 10). Simultaneously with change of spin density the significant change of linewidth of EPR signal is observed. Analyzing the g-factor plot three ranges can be distinguish. In the initial range up to -0.35 V the g-factor value of 2.0026 is constant. At higher potentials g-factor slightly shift to higher values which indicate increase of spin density at S, N or O atoms. Simultaneously  $\Delta B_{pp}$  begins to increase indicated larger localization of radicals. At higher doping level in the measured range results in sharp shift of g-factor up to 2.0031 and further  $\Delta B_{pp}$  increase. The g-factor values of oxidized **poly45** are larger than in **poly1** but lower than in **poly54**. This indicates distinct contribution of oxygen atoms to radical cation orbital however lower than in the case of sulfur atoms.

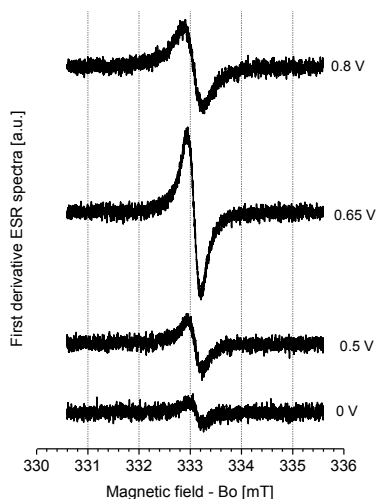


Figure 7 Selected EPR spectra of **poly2** electrodeposited at ITO electrode in 0.1M  $Bu_4NPF_6/ACN$  solution, recorded *in situ* at progressively incremented potentials applied to the film.

UV-Vis-NIR spectra

UV-Vis-NIR absorption difference

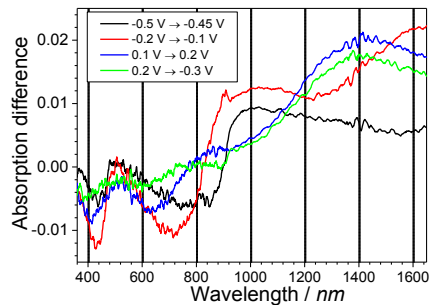
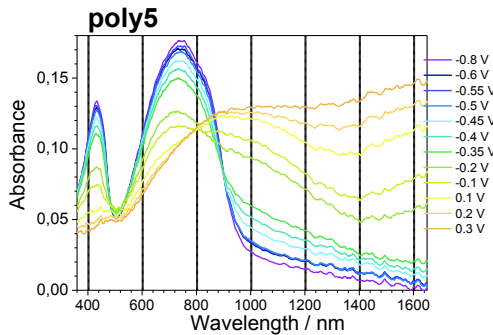
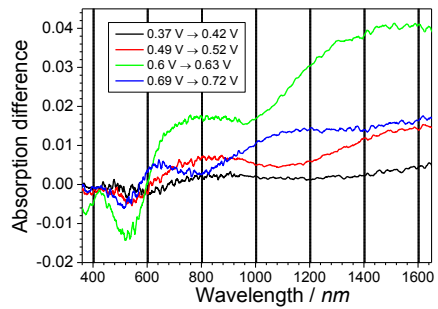
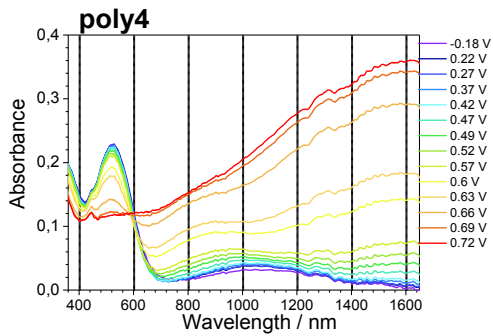
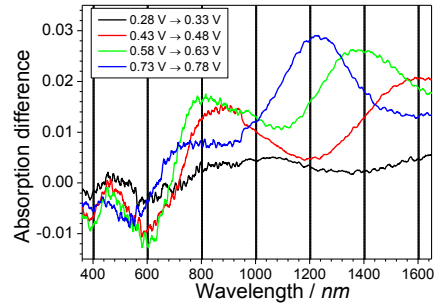
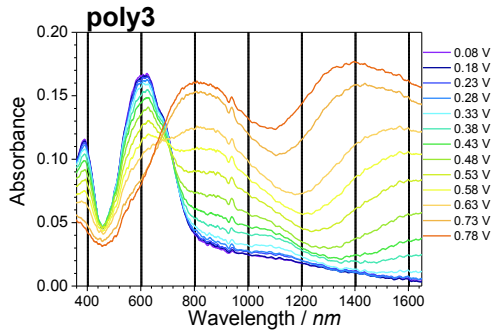
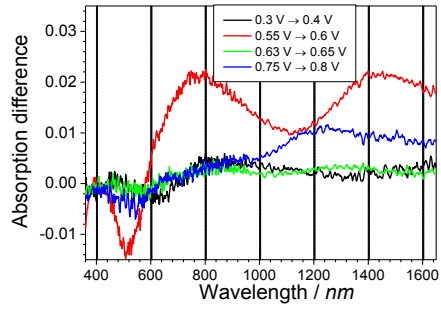
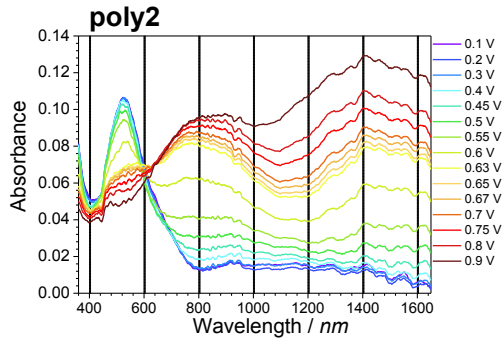
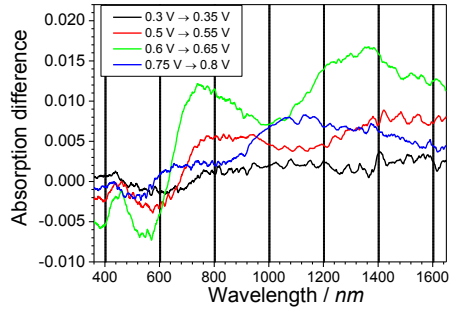
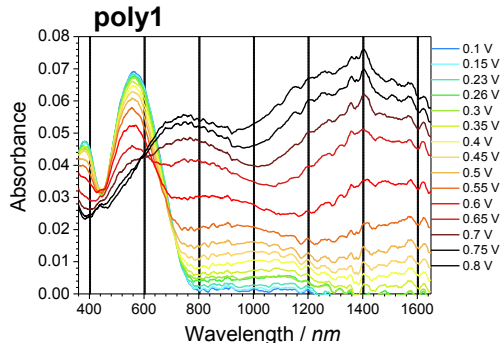




Figure 8 Selected UV-Vis-NIR spectra (left) and their differential spectra (right) of polymer films electrodeposited at ITO electrode in 0.1M Bu<sub>4</sub>NPF<sub>6</sub>/ACN solution, recorded *in situ* at progressively incremented potentials applied to the film.

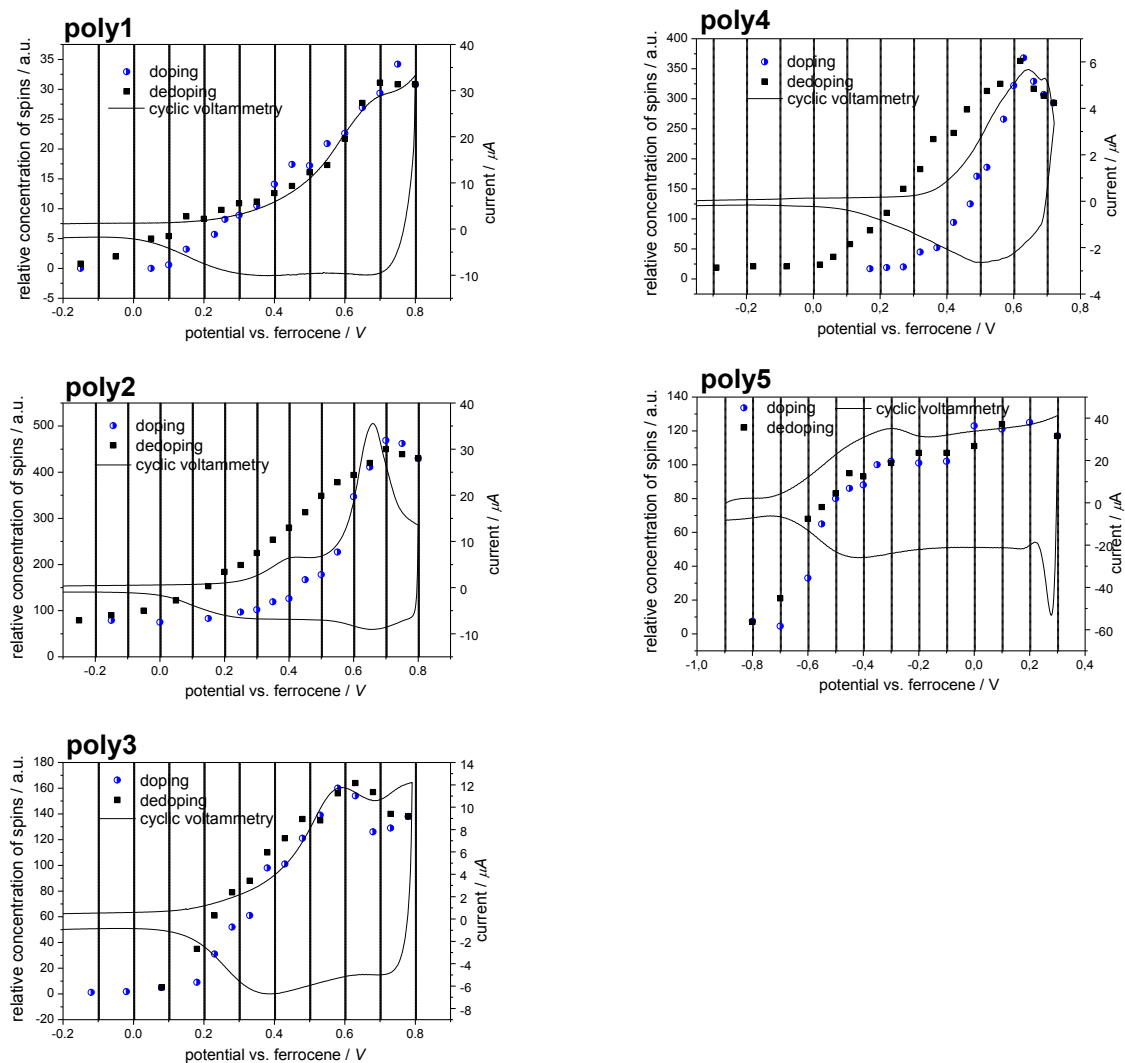


Figure 9 Relative spin concentration and cyclic voltammetry of polymer films in the anodic range.

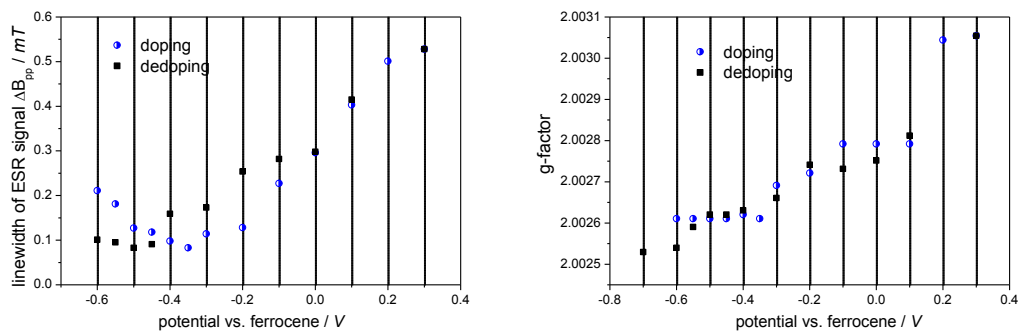


Figure 10 Linewidth of EPR signal and g-factor of **poly45** in the anodic range.

### *n-Doping*

The ESR and UV-Vis-NIR spectra (Figure 11) of studied polymers were also recorded during cathodic doping and dedoping in the potential range related to the first reversible reduction peak at CV. The character of reduction processes is different than oxidation. Already at the beginning of reduction of all studied polymers the signal at EPR appears. Simultaneously UV-Vis-NIR spectra begins to change. New absorption bands appear in the lower energy range. The energy of these new bands appeared during n-doping is different than corresponding absorption bands formed during p-doping. During reduction at applied potential the electrochemical equilibrium at which UV-Vis-NIR and EPR spectra do not present further changes is achieved after longer time. This reach several minutes and depends on the polymer type and thickness of polymer films. In contrary to p-doping UV-Vis-NIR spectra of n-doped species increase homogenously in the whole potential range related to the first reduction peak. No additional transitions are observed at higher doping levels. Simultaneously the appearance of radical anion is confirmed by the formation of Lorentz type of EPR signal. The change of both EPR and UV-Vis-NIR spectra are related to each other. This indicate that only one type of reduced spin-bearing species appears in the n-doped systems.

The g-factor of radical anions is similar for all studied polymers which are 2.0040 – **poly1** and **poly2**, 2.0041 – **poly3**, 2.0042 **poly54** and **poly45**. The strong shift of g-factor value comparing to free radical confirm high spin distribution at heteroatoms. Sulfur and oxygen atoms substituted to the main polymer chain in **poly45** and **poly54** slightly shift g-factor. This indicate delocalization of radical anions mainly at BT unit but also at main polymer chain with sulfur atom of thiophene moiety. The analysis of spectra after n-dedoping reveals charge trapping demonstrated with remaining cation radical transition bands and EPR signal. This issue increases with increased thickness of polymer films.

Comparing of these results with other report [53] presenting irreversible CV of a few BT units linked together in one compounds indicate that not only the LUMO level but also proper balance between donor and acceptor units as well as arrangement and rigidity of polymer structure are

important factors which improve the n-doping ability and electrochemical stability of  $\pi$ -conjugated polymers.

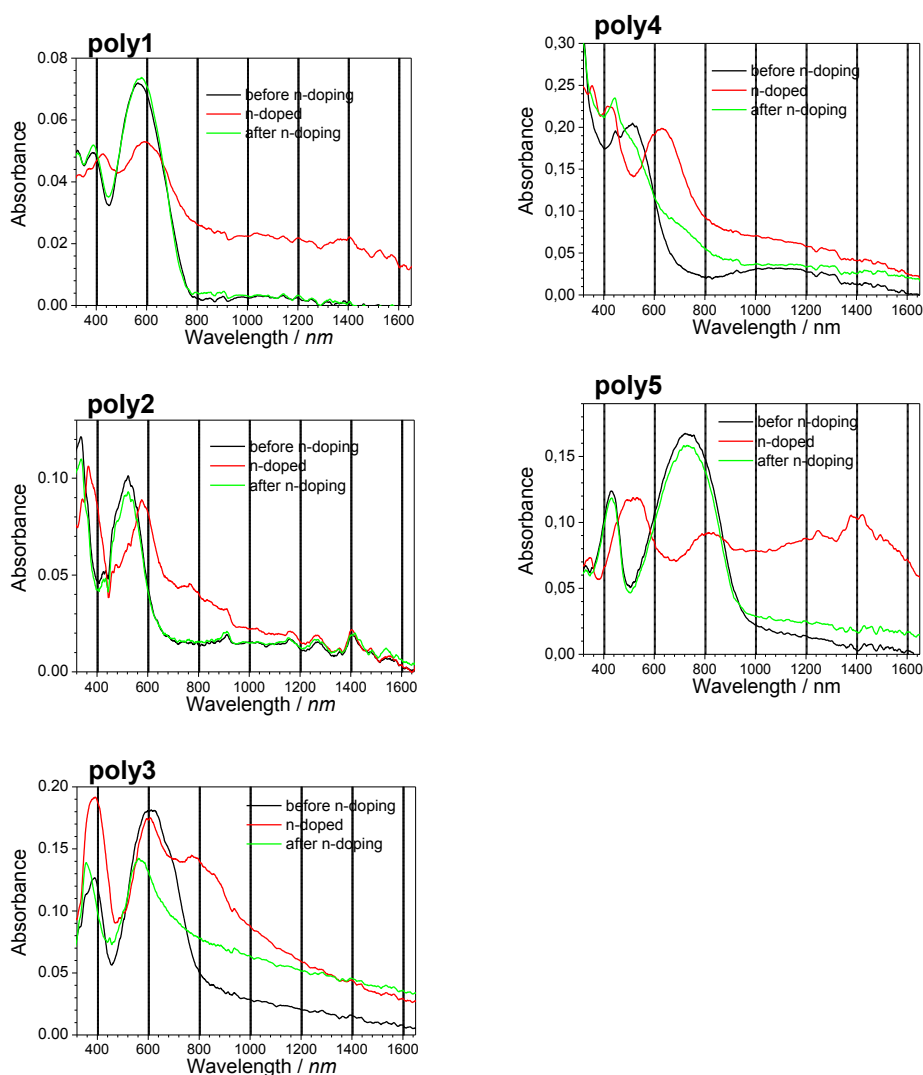


Figure 11 UV-Vis-NIR spectra of polymer films electrodeposited at ITO electrode in 0.1M Bu<sub>4</sub>NPF<sub>6</sub>/ACN solution, recorded at three doped states: neutral state before n-doping, n-doped state, after n-doping in the potential with partial charge trapping.

The comparison of relative spin concentration of **poly45** in p- and n doping range was also made (Figure 12). This polymer film has been chosen own to the best electrochemical stability during n-doping. **Poly45** film was oxidized and then reduced in the same EPR setup and conditions. The ratio between radical anion in the first reduced state and the maximum amount of radical cation exceed 6.2. Assuming that all BT unit undergo reduction the number of spins per unit in p-doping can be also estimated. This indicate the maximum spin concentration as 0.16 spins per monomer unit or 0.053 per

heterocyclic unit. This is lower value compared to 0.12 spin per unit obtained from quantitative measurement of PEDOT.[52]

Spectroelectrochemical and CV analysis show fundamental differences between p- and n-doping. The reduction results with formation of one type charge carrier negative polaron (in the range related to the first reversible redox pair). The oxidation lead to simultaneous formation of different charge carriers positive spin-bearing polaron and spinless species. This different is revealed at CV as broad oxidation band without separated peaks and sharp reduction peak well separated from next reduction step.

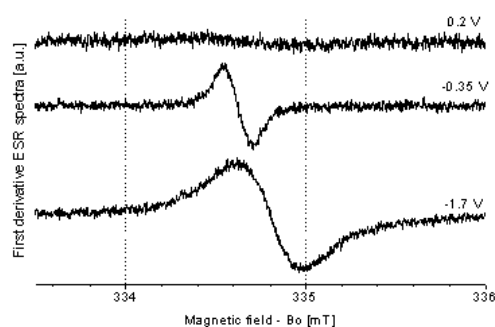


Figure 12 Selected EPR spectra of **poly45** electrodeposited at ITO electrode in 0.1M Bu<sub>4</sub>NPF<sub>6</sub>/ACN solution, recorded *in situ* at different incremented potentials applied to the film. Spectra are shown in restricted range for the clarity.

#### 4. Conclusions

The influence of different thiophene derivatives as donor units with BT as acceptor units were studied for small molecules and polymers. In both cases significant differences were found. Inductive, resonance effect and interatomic interaction leading to flattening of molecules tune the electrochemical and spectroelectrochemical properties. Mainly in the case of EDOT derivative interaction between oxygen and sulfur atoms leads to low band gap polymer with  $E_g^{el} = 1.0$  eV and  $E_g^{op} = 1.26$  eV. Similar effect of reduction of  $E_g$  were weaker for other polymers. The proper balance of different properties of D-A type of  $\pi$ -conjugated organic materials such as HOMO and LUMO level, proper balance between donor and acceptor units, arrangement and rigidity of polymer structure is important factor which improve both p and n-doping.

The comparison of p- and n-doping were made in order to highlight differences between both type of doping. The electrochemical equilibrium of n-doping is achieved after longer time than p-doping reaching several minutes. The clear difference of g-value of negative and positive radicals indicate different contributions of heteroatoms to radical orbital in both states. During reduction in the measured conditions only one type of spin bearing charge carriers was formed in contrary to oxidation

during which different type of spin bearing and spinless charge carriers were found. All these results indicate different mechanism of n- and p- type of electrical conductivity.

## 5. Acknowledgements

This work was financed by Polish National Science Centre grant no. 2011/03/D/ST5/06042.

## 6. References

- [1] Y.H. Wijsboom, Y. Sheynin, A. Patra, N. Zamoshchik, R. Vardimon, G. Leitus, et al., Tuning of electronic properties and rigidity in PEDOT analogs, *J. Mater. Chem.* 21 (2011) 1368–1372. doi:10.1039/c0jm02679d.
- [2] P. Data, M. Lapkowski, R. Motyka, J. Suwinski, Influence of alkyl chain on electrochemical and spectroscopic properties of polyselenophenes, *Electrochim. Acta.* 87 (2013) 438–449. doi:10.1016/j.electacta.2012.09.077.
- [3] J. Mei, Z. Bao, Side chain engineering in solution-processable conjugated polymers, *Chem. Mater.* 26 (2014) 604–615. doi:dx.doi.org/10.1021/cm4020805.
- [4] Z. Gu, L. Deng, H. Luo, X. Guo, H. Li, Z. Cao, et al., Synthesis and photovoltaic properties of conjugated side chains polymers with different electron-withdrawing and donating end groups, *J. Polym. Sci. Part A Polym. Chem.* 50 (2012) 3848–3858. doi:10.1002/pola.26180.
- [5] H. Xie, K. Zhang, C. Duan, S. Liu, F. Huang, Y. Cao, New acceptor-pended conjugated polymers based on 3,6- and 2,7-carbazole for polymer solar cells, *Polymer (Guildf).* 53 (2012) 5675–5683. doi:10.1016/j.polymer.2012.10.008.
- [6] J.A. Schneider, A. Dadvand, W. Wen, D.F. Perepichka, Tuning the Electronic Properties of Poly(thienothiophene vinylene)s via Alkylsulfanyl and Alkylsulfonyl Substituents, *Macromolecules.* 46 (2013) 9231–9239. doi:10.1021/ma402018n.
- [7] L. Yang, J.R. Tumbleston, H. Zhou, H. Ade, W. You, Disentangling the impact of side chains and fluorine substituents of conjugated donor polymers on the performance of photovoltaic blends, *Energy Environ. Sci.* 6 (2013) 316–326. doi:10.1039/c2ee23235a.
- [8] P. Lévêque, L. Biniek, S. Fall, C.L. Chocos, N. Leclerc, T. Heiser, Alkoxy Side Chains in Low Band-Gap Co-Polymers: Impact on Conjugation and Frontier Energy Levels, *Energy Procedia.* 31 (2012) 38–45. doi:10.1016/j.egypro.2012.11.163.
- [9] H.J. Spencer, P.J. Skabara, M. Giles, I. McCulloch, S.J. Coles, M.B. Hursthouse, The first direct experimental comparison between the hugely contrasting properties of PEDOT and the all-sulfur analogue PEDTT by analogy with well-defined EDTT–EDOT copolymers, *J. Mater. Chem.* 15 (2005) 4783–4792. doi:10.1039/b511075k.
- [10] J. Roncali, P. Blanchard, P. Frère, 3,4-Ethylenedioxythiophene (EDOT) as a versatile building block for advanced functional  $\pi$ -conjugated systems, *J. Mater. Chem.* 15 (2005) 1589–1610. doi:10.1039/b415481a.
- [11] W. Domagala, D. Palutkiewicz, D. Cortizo-Lacalle, A.L. Kanibolotsky, P.J. Skabara, Redox doping behaviour of poly(3,4-ethylenedithiophene) – The counterion effect, *Opt. Mater. (Amst).* 33 (2011) 1405–1409. doi:10.1016/j.optmat.2011.02.030.
- [12] J. Chen, Y. Cao, Development of novel conjugated donor polymers for high-efficiency bulk-heterojunction photovoltaic devices., *Acc. Chem. Res.* 42 (2009) 1709–18. doi:10.1021/ar900061z.

- [13] E.N. Esmer, S. Tarkuc, Y.A. Udum, L. Toppare, Near infrared electrochromic polymers based on phenazine moieties, *Mater. Chem. Phys.* 131 (2011) 519–524. doi:10.1016/j.matchemphys.2011.10.014.
- [14] Z. Li, Y. Zhang, A.L. Holt, B.P. Kolasa, J.G. Wehner, A. Hampp, et al., Electrochromic devices and thin film transistors from a new family of ethylenedioxythiophene based conjugated polymers, *New J. Chem.* 35 (2011) 1327. doi:10.1039/c0nj00837k.
- [15] P.M. Beaujuge, S. Ellinger, J.R. Reynolds, Spray Processable Green to Highly Transmissive Electrochromics via Chemically Polymerizable Donor-Acceptor Heterocyclic Pentamers, *Adv. Mater.* 20 (2008) 2772–2776. doi:10.1002/adma.200800280.
- [16] Z. Zhang, J. Wang, Structures and properties of conjugated Donor–Acceptor copolymers for solar cell applications, *J. Mater. Chem.* 22 (2012) 4178–4187. doi:10.1039/c2jm14951f.
- [17] E. Poverenov, N. Zamoshchik, A. Patra, Y. Ridelman, M. Bendikov, Unusual doping of donor-acceptor-type conjugated polymers using lewis acids., *J. Am. Chem. Soc.* 136 (2014) 5138–5149. doi:10.1021/ja501024n.
- [18] Y.-H. Chen, L.-Y. Lin, C.-W. Lu, F. Lin, Z.-Y. Huang, H.-W. Lin, et al., Vacuum-deposited small-molecule organic solar cells with high power conversion efficiencies by judicious molecular design and device optimization., *J. Am. Chem. Soc.* 134 (2012) 13616–13623. doi:10.1021/ja301872s.
- [19] M.L. Keshtov, D. V Marochkin, V.S. Kochurov, A.R. Khokhlov, E.N. Koukaras, G.D. Sharma, New conjugated alternating benzodithiophene-containing copolymers with different acceptor units: synthesis and photovoltaic application, *J. Mater. Chem. A.* 2 (2014) 155–171. doi:10.1039/C3TA12967E.
- [20] S. Tarkuc, E.K. Unver, Y.A. Udum, L. Toppare, Multi-colored electrochromic polymer with enhanced optical contrast, *Eur. Polym. J.* 46 (2010) 2199–2205. doi:10.1016/j.eurpolymj.2010.08.002.
- [21] S. Ozdemir, M. Sendur, G. Oktem, Ö. Doğan, L. Toppare, A promising combination of benzotriazole and quinoxaline units: A new acceptor moiety toward synthesis of multipurpose donor–acceptor type polymers, *J. Mater. Chem.* 22 (2012) 4687–4694. doi:10.1039/c2jm16171k.
- [22] K. Takimiya, I. Osaka, M. Nakano,  $\pi$ -Building Blocks for Organic Electronics: Reevaluation of “Inductive” and “Resonance” Effects of  $\pi$ -Electron Deficient Units, *Chem. Mater.* 26 (2014) 587–593. doi:10.1021/cm4021063.
- [23] J.-C. Li, S.-J. Kim, S.-H. Lee, Y.-S. Lee, K. Zong, S.-C. Yu, Synthesis and characterization of a thiophene-benzothiadiazole copolymer, *Macromol. Res.* 17 (2009) 356–360. doi:10.1007/BF03218875.
- [24] M. Sendur, A. Balan, D. Baran, B. Karabay, L. Toppare, Combination of donor characters in a donor–acceptor–donor (DAD) type polymer containing benzothiadiazole as the acceptor unit, *Org. Electron.* 11 (2010) 1877–1885. doi:10.1016/j.orgel.2010.09.001.
- [25] H. Shang, H. Fan, Y. Liu, W. Hu, Y. Li, X. Zhan, A solution-processable star-shaped molecule for high-performance organic solar cells., *Adv. Mater.* 23 (2011) 1554–1557. doi:10.1002/adma.201004445.
- [26] Y. Jiang, D. Yu, L. Lu, C. Zhan, D. Wu, W. You, et al., Tuning optical and electronic properties of star-shaped conjugated molecules with enlarged  $\pi$ -delocalization for organic solar cell application, *J. Mater. Chem. A.* 1 (2013) 8270–8279. doi:10.1039/c3ta11001j.
- [27] B. Fu, J. Baltazar, A.R. Sankar, P.-H. Chu, S. Zhang, D.M. Collard, et al., Enhancing Field-Effect Mobility of Conjugated Polymers Through Rational Design of Branched Side Chains, *Adv. Funct. Mater.* 24 (2014) 3734–3744. doi:10.1002/adfm.201304231.

- [28] A.A. El-Shehawy, N.I. Abdo, A.A. El-Barbary, J.-S. Lee, Alternating Copolymers Based on 2,1,3-Benzothiadiazole and Hexylthiophene: Positioning Effect of Hexyl Chains on the Photophysical and Electrochemical Properties, *European J. Org. Chem.* 2011 (2011) 4841–4852. doi:10.1002/ejoc.201100182.
- [29] M. Scarongella, A. Laktionov, U. Rothlisberger, N. Banerji, Charge transfer relaxation in donor-acceptor type conjugated materials, *J. Mater. Chem. C* 1 (2013) 2308–2319. doi:10.1039/C3TC00829K.
- [30] P.J. Skabara, R. Berridge, I.M. Serebryakov, A.L. Kanibolotsky, L. Kanibolotskaya, S. Gordeyev, et al., Fluorene functionalised sexithiophenes?utilising intramolecular charge transfer to extend the photocurrent spectrum in organic solar cells, *J. Mater. Chem.* 17 (2007) 1055–1062. doi:10.1039/b609858d.
- [31] S. Pelz, J. Zhang, I. Kanelidis, D. Klink, L. Hyzak, V. Wulf, et al., Synthesis and Characterization of Star-Shaped Donor–Acceptor–Donor Structures, *European J. Org. Chem.* 2013 (2013) 4761–4769. doi:10.1002/ejoc.201300357.
- [32] A. Durmus, G.E. Gunbas, L. Toppare, New, Highly Stable Electrochromic Polymers from 3,4-Ethylenedioxythiophene–Bis-Substituted Quinoxalines toward Green Polymeric Materials, *Chem. Mater.* 19 (2007) 6247–6251. doi:10.1021/cm702143c.
- [33] A. Durmus, G.E. Gunbas, P. Camurlu, L. Toppare, A neutral state green polymer with a superior transmissive light blue oxidized state., *Chem. Commun. (Camb)*. (2007) 3246–3248. doi:10.1039/b704936f.
- [34] B. Aydogan, G.E. Gunbas, A. Durmus, L. Toppare, Y. Yagci, Highly Conjugated Thiophene Derivatives as New Visible Light Sensitive Photoinitiators for Cationic Polymerization, *Macromolecules*. 43 (2010) 101–106. doi:10.1021/ma901858p.
- [35] S. Göker, G. Hızalan, Y.A. Udum, L. Toppare, Electrochemical and optical properties of 5,6-bis(octyloxy)-2,1,3 benzooxadiazole containing low band gap polymers, *Synth. Met.* 191 (2014) 19–27. doi:10.1016/j.synthmet.2014.02.010.
- [36] J. Roncali, Conjugated poly(thiophenes): synthesis, functionalization, and applications, *Chem. Rev.* 92 (1992) 711–738. doi:10.1021/cr00012a009.
- [37] G.R. Eaton, S.S. Eaton, D.P. Barr, R.T. Weber, *Quantitative EPR*, Springer Vienna, Vienna, 2010. doi:10.1007/978-3-211-92948-3.
- [38] J. Gierschner, J. Cornil, H.-J. Egelhaaf, Optical Bandgaps of  $\pi$ -Conjugated Organic Materials at the Polymer Limit: Experiment and Theory, *Adv. Mater.* 19 (2007) 173–191. doi:10.1002/adma.200600277.
- [39] A. Mirloup, N. Leclerc, S. Rihn, T. Bura, R. Bechara, A. Hebraud, et al., A deep-purple-grey thiophene-benzothiadiazole-thiophene BODIPY dye for solution-processed solar cells, *New J. Chem.* (2014) -. doi:10.1039/C4NJ00294F.
- [40] J. Pina, J.S. de Melo, D. Breusov, U. Scherf, Donor-acceptor-donor thienyl/bithienyl-benzothiadiazole/quinoxaline model oligomers: experimental and theoretical studies, *Phys. Chem. Chem. Phys.* 15 (2013) 15204–15213. doi:10.1039/C3CP52056K.
- [41] E. Ripaud, Y. Olivier, P. Leriche, J. Cornil, J. Roncali, Polarizability and Internal Charge Transfer in Thiophene–Triphenylamine Hybrid  $\pi$ -Conjugated Systems, *J. Phys. Chem. B*. 115 (2011) 9379–9386. doi:10.1021/jp203759e.
- [42] Z. Chen, J. Fang, F. Gao, T.J.K. Brenner, K.K. Banger, X. Wang, et al., Enhanced charge transport by incorporating additional thiophene units in the poly(fluorene-thienyl-benzothiadiazole) polymer, *Org. Electron.* 12 (2011) 461–471. doi:10.1016/j.orgel.2010.12.009.
- [43] J.Y. Lee, S.W. Heo, H. Choi, Y.J. Kwon, J.R. Haw, D.K. Moon, Synthesis and characterization of 2,1,3-benzothiadiazole-thieno[3,2-b]thiophene-based charge transferred-type polymers for

- photovoltaic application, *Sol. Energy Mater. Sol. Cells.* 93 (2009) 1932–1938.  
doi:10.1016/j.solmat.2009.07.006.
- [44] J. Tsutsumi, H. Matsuzaki, N. Kanai, T. Yamada, T. Hasegawa, Charge Separation and Recombination of Charge-Transfer Excitons in Donor–Acceptor Polymer Solar Cells, *J. Phys. Chem. C.* 117 (2013) 16769–16773. doi:10.1021/jp404094e.
- [45] C. Deibel, T. Strobel, V. Dyakonov, Role of the Charge Transfer State in Organic Donor–Acceptor Solar Cells, *Adv. Mater.* 22 (2010) 4097–4111. doi:10.1002/adma.201000376.
- [46] J. Heinze, B. a Frontana-Urbe, S. Ludwigs, Electrochemistry of conducting polymers--persistent models and new concepts., *Chem. Rev.* 110 (2010) 4724–4771.  
doi:10.1021/cr900226k.
- [47] I. Osaka, M. Shimawaki, H. Mori, I. Doi, E. Miyazaki, T. Koganezawa, et al., Synthesis, Characterization, and Transistor and Solar Cell Applications of a Naphthobisthiadiazole-Based Semiconducting Polymer, *J. Am. Chem. Soc.* 134 (2012) 3498–3507. doi:10.1021/ja210687r.
- [48] D. Fichou, *Handbook of Oligo- and Polythiophenes*, Wiley-VCH, Weinheim, 1999.
- [49] T. Nishinaga, K. Komatsu, Persistent [small pi] radical cations: self-association and its steric control in the condensed phase, *Org. Biomol. Chem.* 3 (2005) 561–569.  
doi:10.1039/B418872A.
- [50] Y. Yu, E. Gunic, B. Zinger, L.L. Miller, Spectra and Reactivity of Methoxyoligothiophene Cation Radicals, *J. Am. Chem. Soc.* 118 (1996) 1013–1018. doi:10.1021/ja9533104.
- [51] J.L. Bredas, G.B. Street, Polarons, bipolarons, and solitons in conducting polymers, *Acc. Chem. Res.* 18 (1985) 309–315. doi:10.1021/ar00118a005.
- [52] W. Domagala, B. Pilawa, M. Lapkowski, Quantitative in-situ EPR spectroelectrochemical studies of doping processes in poly(3,4-alkylenedioxythiophene)s, *Electrochim. Acta.* 53 (2008) 4580–4590. doi:10.1016/j.electacta.2007.12.068.
- [53] E. Xu, H. Zhong, J. Du, D. Zeng, S. Ren, J. Sun, et al., The synthesis and properties of novel  $\pi$ -conjugated 2,1,3-benzothiadiazole oligomers, *Dye. Pigment.* 80 (2009) 194–198.  
doi:10.1016/j.dyepig.2008.07.008.